

Graph Transformers without Positional Encodings

Ayush Garg*

ayush.garg@alumni.ethz.ch

Abstract

Recently, Transformers for graph representation learning have become increasingly popular, achieving state-of-the-art performance on a wide-variety of datasets, either alone or in combination with message-passing graph neural networks (MP-GNNs). Infusing graph inductive-biases in the innately structure-agnostic transformer architecture in the form of structural or positional encodings (PEs) is key to achieving these impressive results. However, designing such encodings is tricky and disparate attempts have been made to engineer such encodings including Laplacian eigenvectors, relative random-walk probabilities (RRWP), spatial encodings, centrality encodings, edge encodings etc. In this work, we argue that such encodings may not be required at all, provided the attention mechanism itself incorporates information about the graph structure. We introduce Eigenformer, a Graph Transformer employing a novel *spectrum-aware* attention mechanism cognizant of the Laplacian spectrum of the graph, and empirically show that it achieves performance comparable to SOTA Graph Transformers on a number of standard GNN benchmark datasets, even surpassing the SOTA on some datasets. The simpler attention mechanism also allows us to train wider and deeper models for a given parameter budget.

1 Introduction

Learning from graph data is useful in a variety of domains due to the ubiquitous presence of graphs around us, ranging from molecules to social networks and transportation networks. It may well be argued that "graphs are the main modality of data we receive from nature" [Veličković, 2023]. In general machine learning methods designed to learn patterns in graph data fall into two paradigms: message-passing graph neural networks (MP-GNNs), where vector messages are exchanged between neighboring nodes and updated using neural networks [Bruna et al., 2014, Gilmer et al., 2017], and more recently Transformers [Vaswani et al., 2017] –originally designed for Natural Language Processing (NLP) tasks– for graph data, which feature long-range connections between nodes for faster information exchange albeit with a loss of graph inductive biases [Dwivedi and Bresson, 2020, Kreuzer et al., 2021, Chen et al., 2022a, Ying et al., 2021, Rampášek et al., 2022, Hussain et al., 2022, Zhang et al., 2023].

In many ways, MP-GNNs and Graph Transformers have complementary strengths and weaknesses. While MP-GNNs have strong graph inductive biases due to sharing of messages within local neighborhoods, they suffer from issues such as over-squashing [Alon and Yahav, 2021, Topping et al., 2022], over-smoothing [Li et al., 2018, Oono and Suzuki, 2020] and expressivity concerns (upper bounded by the 1-Weisfeiler-Lehman isomorphism test) [Xu et al., 2019, Loukas, 2020, Morris et al., 2019]. On the other hand, Graph Transformers do not suffer from these issues, at the expense of lacking graph inductive biases (forgoing locality with usually all-to-all connectivity between nodes), possibility of over-fitting and quadratic computational and memory complexity. Due to their complementary benefits, researchers have (successfully) tried to merge the two paradigms together into one architecture with GraphGPS in Rampášek et al. [2022].

*Independent research

A common weakness in both methods however, is the lack of positional information of nodes, which has been shown to be crucial both to improve expressivity in MP-GNNs (as compared to the 1-WL test in Xu et al. [2019]) and to allow Transformers to be used with small-scale graph data. Nodes in a graph innately lack a canonical order, and superficially imposing an ordering leads to exponential growth in possible such orderings, leading to learning difficulties. To tackle this, PEs based on Laplacian eigenvectors were proposed in Dwivedi and Bresson [2020]. Due to sign ambiguities of eigenvectors and eigenvalue multiplicities, sign and basis invariant/equivariant methods such as SignNet and BasisNet in Lim et al. [2023] were proposed. In other works [Dwivedi et al., 2022a, Ma et al., 2023], k-dimensional (learnable) random-walk probabilities from a node to itself are used instead of Laplacian eigenvectors to avoid the aforementioned invariance issues.

Contributions: In light of the above background, we ask the question whether such encodings are indeed necessary at all. If there is no canonical node-ordering inherent to a graph, perhaps no such ordering is required to effectively learn patterns in graph data. Thus, in this work, we seek to circumvent the issues related to designing node/edge PEs by modifying the way node feature information is exchanged in a Graph Transformer. Specifically:

- Instead of adding positional information to node features and letting the attention mechanism figure out the strength of connection between a pair of nodes, we factorize the attention matrix in terms of fixed spectral similarities and learned frequency importances. We posit such a factorization encodes important graph inductive biases from the frequency domain into the attention mechanism, while being flexible enough to yield impressive performance across domains and objectives.
- We utilize valuable information from both the eigenvectors and the eigenvalues as advocated in Kreuzer et al. [2021], forgoing the assumption that higher frequencies are less important in determining node similarity.
- The novel attention mechanism with built-in inductive biases allows us to train deeper models for a given parameter budget due to simpler Transformer layers. Numerical experiments demonstrate the strength of our method, achieving near-SOTA performances on many common GNN benchmarks.

2 Related Work

Graph connectivity and graph topology information can be very important for a GNN architecture, and following the introduction of Graph Transformers in Li et al. [2019], there have been many attempts to incorporate graph structural information in Transformers.

Graph inductive biases in Transformers Dwivedi and Bresson [2020] perform attention only over the 1-hop neighborhood of nodes in addition to the use of Laplacian eigenvectors as node PEs. With Graph-BERT, Zhang et al. [2020] propose to train Transformers using sampled linkless (no edges) subgraphs within their local contexts, designed with an emphasis on parallelization and mainly as a pretraining technique. They use a number of PEs like the WL Absolute Role Embedding, Intimacy based Relative Positional Embedding and Hop based Relative Distance Embedding, in order to retain the original graph structural information in the linkless subgraphs.

Kreuzer et al. [2021] use a Transformer encoder to create learnable PEs from a combination of eigenvalues and eigenvectors which are then fed to the main Transformer network. Dwivedi et al. [2022a] decouple the node features and the node PEs with a separate propagation step for the PEs. They consider two different initializations for the PEs: Laplacian PE (LapPE) and Random Walk PE (RWPE), and show that RWPE outperforms LapPE, indicating that learning the sign invariance ambiguity in LapPE is more difficult than not exactly having unique node representation for each node. Ying et al. [2021] propose the use of a fixed centrality encoding to inject degree information in their Graphormer.

With GraphiT, Mialon et al. [2021] enumerate, encode and aggregate local sub-structures such as paths of length-k using Graph convolutional kernel networks (GCKN) [Chen et al., 2020] to create node PEs. Ma et al. [2023] propose GRIT, again using PEs initialized with random walk probabilities but make them flexible and learnable by composing with an MLP, and provide theoretical proof of the expressivity of such a composition. Further, they inject degree information using an adaptive

degree-scaler [Corso et al., 2020] in every layer, noting that attention mechanisms are invariant to node-degrees.

Structure-aware attention mechanisms More similar to our work, there has also been research on creating structure-aware attention mechanisms in order to infuse node structural and neighborhood similarity information. Mialon et al. [2021] view self-attention as kernel smoothing and bias the attention scores using diffusion or k-step random-walk kernels. Chen et al. [2022b] argue that such a modification is deficient in filtering out structurally dissimilar nodes, and consider a more generalized kernel accounting for local substructures like k-subtrees and k-subgraphs, around each node. In a similar approach, G et al. [2023] aggregate node feature information from k-subtrees but augment their transformer with a global node and train positional encodings using the Neighbourhood Contrastive Loss (NCE). Ying et al. [2021] have proposed to inject spatial and edge information by adding learnable encodings to the attention scores before normalization, while [Menegaux et al., 2023] augment that idea further by learning a different attention score per hidden dimension in their so-called Chromatic Self-Attention. Learned edge encodings are also incorporated in Hussain et al. [2022] both as a bias to the attention score before normalization and as a sigmoid-gate after normalization.

In contrast to previous work, to the best of our knowledge, there have been no attempts to factorize the attention matrix into spectral similarities and frequency importances, which we present in detail in the next section.

3 Methodology and Theory

In this section, we introduce our novel *spectrum-aware* attention (SAA) mechanism and its use in the proposed Eigenformer architecture. We first present the motivation behind the architecture by reproducing the meaning of the graph Laplacian and its spectrum.

3.1 Graph Laplacian and its spectrum

For an undirected graph $\mathcal{G} = (\mathcal{V}, \mathcal{E})$, the unnormalized graph Laplacian L is defined as

$$L = D - A \quad (1)$$

where A is the adjacency matrix and D is the degree matrix.

By the Rayleigh-Ritz theorem, the eigenvectors $u_i, i = 1, \dots, |\mathcal{V}|$ of the Laplacian solve the problems:

$$\operatorname{argmin}_{u_i \in \mathbb{R}^{|\mathcal{V}|}: u_i \perp u_j \forall j < i} \frac{u_i^T L u_i}{u_i^T u_i} \quad (2)$$

and the values attained are the eigenvalues $\lambda_i, i = 1, \dots, |\mathcal{V}|$.

By definition 1, the following is also true for a unit-norm eigenvector u_i and its corresponding eigenvalue λ_i :

$$\lambda_i = u_i^T L u_i = \frac{1}{2} \sum_{u,v \in \mathcal{V}} A[u,v] (u_i[u] - u_i[v])^2 = \sum_{(u,v) \in \mathcal{E}} (u_i[u] - u_i[v])^2 \quad (3)$$

If the eigenvectors are interpreted as "signals" over the graph, taking real scalar values at nodes, then the eigenvalues act as a measure of the "smoothness" of such signals over the graph, measuring how much the signal values differ between endpoints of edges. The smallest eigenvalue is always 0, assigning the same scalar value $u_i[\cdot]$ to all nodes in the same connected component of the graph.

As discussed in previous works (eg. Kreuzer et al. [2021]), the Laplacian spectrum equates to sine functions over graphs and encodes important information about relative distances between nodes. Nodes close to each other tend to have similar values under a given eigenvector. As such, the spectrum—in its interpretation as frequencies of resonance of the graph—discriminates between different graph structures and sub-structures. Figure 1 shows substructures revealed by eigenvectors for an example graph from the ZINC dataset containing 33 nodes. Color-coded nodes indicate the value $u_i[\cdot]$ for different frequencies λ_i where $i \in [0, 32]$.

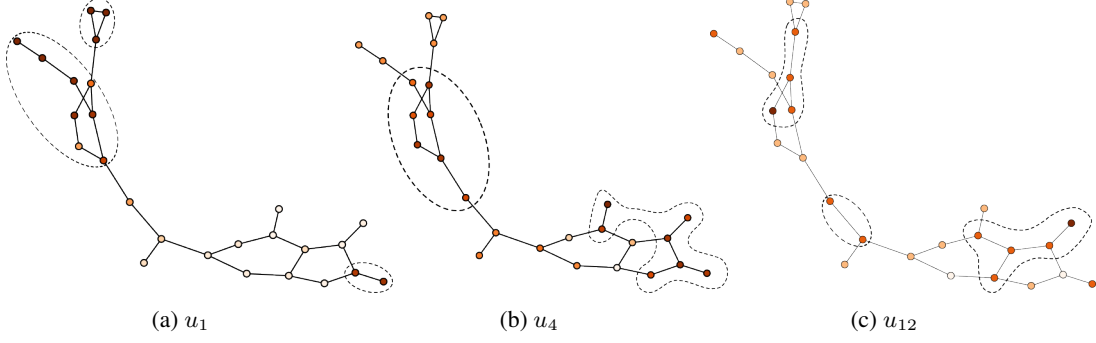


Figure 1: ZINC dataset: Graph substructures revealed by the eigenvectors

There is also a normalized variant of the graph Laplacian, $L_{sym} = D^{-\frac{1}{2}} L D^{-\frac{1}{2}}$ that admits similar properties and interpretations of the spectrum as that of L , but has better numerical stability due to bounded spectrum: all eigenvalues of L_{sym} lie between 0 and 2. Moreover, the normalized Laplacian counters the effect of "heavy" nodes (nodes with high degrees) in influencing information propagation through the graph. We propose to use the spectrum of L_{sym} to define a new spectrum-aware attention mechanism as outlined in the next section.

3.2 Attention using the Laplacian spectrum

We define the attention weight between two nodes i and j through the following equations:

$$\sigma_k[i, j] = u_k[i] \cdot u_k[j] \quad (4)$$

$$\alpha[i, j] = \text{softmax}_{j \in \mathcal{V}} \left[\phi_1 \left(\sum_{k=1}^{|\mathcal{V}|} \sigma_k[i, j] \phi_2(\lambda_k) \right) \right] \quad (5)$$

where u_k is the eigenvector corresponding to the eigenvalue λ_k of L_{sym} , σ_k is assumed to measure the similarity between nodes "under" the frequency λ_k , ϕ_1 and ϕ_2 are arbitrary functions and α is the final attention weight.

The matrices $\sigma_k[\cdot, \cdot]$ for $k = 1 \dots |\mathcal{V}|$ can be thought of as defining $|\mathcal{V}|$ "eigen-similarity" matrices measuring the strength of connection between pairs of nodes under different frequencies. Nodes simultaneously having high values and same sign of $u_k[\cdot]$ are deemed to be more correlated under that frequency. The justification for this choice of σ_k is presented in Proposition 1 below (proof in Appendix A).

Proposition 1 For any $n \in \mathbb{N}$, consider the symmetric adjacency matrix A drawn from the set of adjacency matrices of n -node undirected graphs, $\mathbb{G}_n \subset \{0, 1\}^{n \times n}$. Further, let $L_{sym} = I - D^{-\frac{1}{2}} A D^{-\frac{1}{2}} = I - A_{sym}$ be the normalized graph Laplacian of the graph $\mathcal{G} = (\mathcal{V}, \mathcal{E})$ with adjacency matrix A , eigenvalues λ_k and eigenvectors u_k for $k \in [1, |\mathcal{V}|]$ with $|\mathcal{V}| = n$. Then, we have the following approximations upto an arbitrary small error ϵ :

1. $\phi_1 \left(\sum_{k=1}^{|\mathcal{V}|} \sigma_k[i, j] \cdot \phi_2(\lambda_k) \right) \approx \sum_{k=0}^m \theta_k A_{sym}^k[i, j]$ for $m \in \mathbb{Z}$
2. $\phi_1 \left(\sum_{k=1}^{|\mathcal{V}|} \sigma_k[i, j] \cdot \phi_2(\lambda_k) \right) \approx SPD[i, j]$

for suitable functions ϕ_1 and ϕ_2 , where $SPD[i, j]$ is the shortest path distance between nodes i and j .

Proposition 1 states that the attention mechanism defined in 5 can capture (i) shortest path distances between all pairs of nodes and (ii) all weighted combinations of powers of the normalized adjacency matrix A_{sym} allowing us to perform aggregations over any k -hop neighborhood where $k \in \mathbb{N}$. The

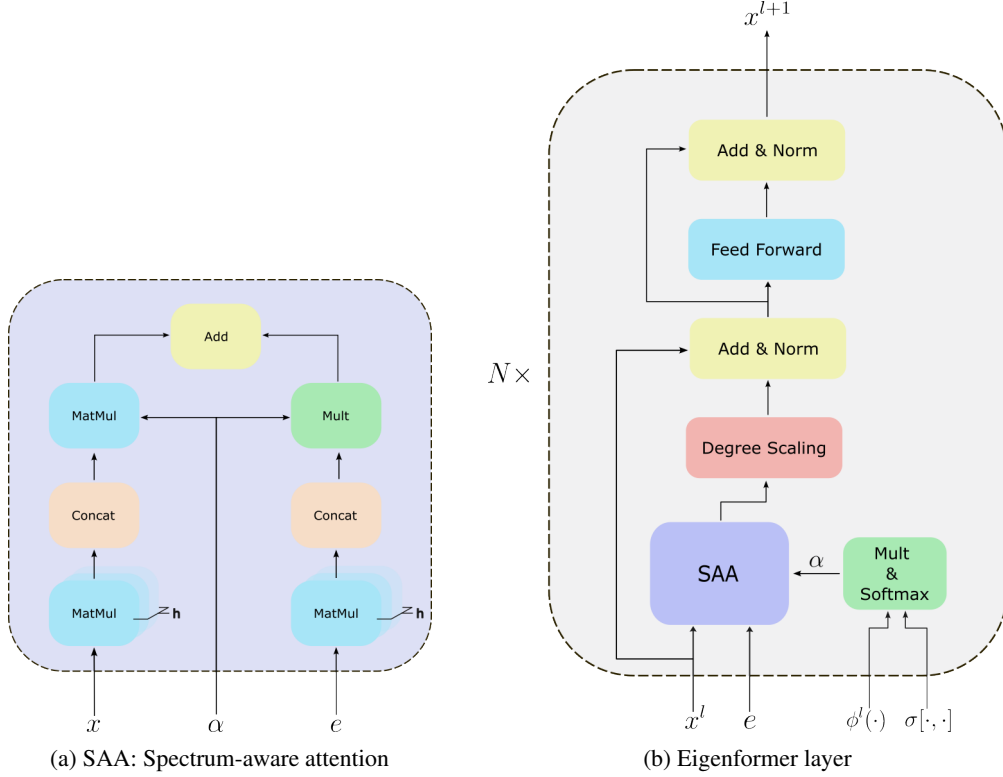


Figure 2: Eigenformer Architecture

function ϕ_2 quantifies the importance of the frequency λ_k in the sum in 5, deciding how to mix the $|\mathcal{V}|$ eigen-similarity matrices to obtain node connection strengths that are useful for the graph learning task at hand. Traditional distance metrics like the biharmonic distance [Lipman et al., 2010] or the diffusion distance [Coifman and Lafon, 2006, Bronstein et al., 2017], weigh smaller frequencies more heavily, assuming that higher frequencies play a smaller role in the measurement of relative distance between nodes. We make no such assumption, rather allowing the dependence on the frequency to be learnt from data by parameterizing the function ϕ_2 appropriately.

Note that calculation of the similarities in 4 is possible offline with just the graph adjacency matrix A whereas 5 requires us to choose the form of ϕ_1 and ϕ_2 . Thus, the only learnable components in our proposed method are the functions ϕ_1 and ϕ_2 , leading to a drastic simplification of the attention mechanism.

3.3 Eigenformer Architecture

For a layer l of the transformer, input node features $x_i^l \in \mathbb{R}^{d_v}$ for $i = 1, \dots, |\mathcal{V}|$ and input edge features $e_{ij} \in \mathbb{R}^{d_e}$ for $i, j = 1, \dots, |\mathcal{V}|$, the node feature propagation is performed using:

$$\alpha^l[i, j] = \text{softmax}_{j \in \mathcal{V}} \left[\phi_1^l \left(\sum_{k=1}^{|\mathcal{V}|} \sigma_k[i, j] \phi_2^l(\lambda_k) \right) \right] \quad (6)$$

$$\hat{x}_i^{l+1} = \sum_{j \in \mathcal{V}} \alpha^l[i, j] \cdot \prod_{h=1}^H (W_{h, \mathcal{V}}^l x_j^l + W_{h, \mathcal{E}}^l e_{ij}) \quad (7)$$

$$\tilde{x}_i^{l+1} = \hat{x}_i^{l+1} \odot \theta_1 + \log(1 + d_i) \cdot \hat{x}_i^{l+1} \odot \theta_2 \quad (8)$$

$$x_i'^{l+1} = \text{BN}(x_i^l + \tilde{x}_i^{l+1}) \quad (9)$$

Table 1: Test performance on four benchmarks from Dwivedi et al. [2020]. Due to limited training budget, we only show our results for a single training run while other baselines report mean \pm standard deviation numbers of 4 runs with different random seeds. Color codes denote top **first**, **second**, **third** results.

| Model | ZINC | MNIST | PATTERN | CLUSTER |
|--------------------|----------------------------------|-----------------------------------|-----------------------------------|-----------------------------------|
| | MAE \downarrow | Accuracy \uparrow | Accuracy \uparrow | Accuracy \uparrow |
| GCN | 0.367 \pm .011 | 90.705 \pm .218 | 71.892 \pm .334 | 68.498 \pm .976 |
| GIN | 0.526 \pm .051 | 96.485 \pm .252 | 85.387 \pm .136 | 64.716 \pm 1.553 |
| GAT | 0.384 \pm .007 | 95.535 \pm .205 | 78.271 \pm .186 | 70.587 \pm .447 |
| GatedGCN | 0.282 \pm .015 | 97.340 \pm .143 | 85.568 \pm .088 | 73.840 \pm .326 |
| GatedGCN-LSPE | 0.090 \pm .001 | - | - | - |
| PNA | 0.188 \pm .004 | 97.940 \pm .12 | - | - |
| DGN | 0.168 \pm .003 | - | 86.680 \pm .034 | - |
| GSN | 0.101 \pm .010 | - | - | - |
| CIN | 0.079\pm.006 | - | - | - |
| CRaW1 | 0.085 \pm .004 | 97.944 \pm .050 | - | - |
| GIN-AK+ | 0.080 \pm .001 | - | 86.850\pm.057 | - |
| SAN | 0.139 \pm .006 | - | 86.581 \pm .037 | 76.691 \pm .65 |
| Graphormer | 0.122 \pm .006 | - | - | - |
| K-Subgraph SAT | 0.094 \pm .008 | - | 86.848 \pm .037 | 77.856 \pm .104 |
| EGT | 0.108 \pm .009 | 98.173\pm.087 | 86.821 \pm .020 | 79.232\pm.348 |
| Graphormer-URPE | 0.086 \pm .007 | - | - | - |
| Graphormer-GD | 0.081 \pm .009 | - | - | - |
| GPS | 0.070\pm.004 | 98.051 \pm .126 | 86.685 \pm .059 | 78.016 \pm .180 |
| GRIT | 0.059\pm.002 | 98.108\pm.111 | 87.196\pm.076 | 80.026\pm.277 |
| EXPHORMER | - | 98.55\pm.039 | 86.740 \pm .015 | 78.070\pm.037 |
| Eigenformer (ours) | 0.104 | 96.178 | 90.761 | 76.683 |

$$x_i^{l+1} = BN(x_i'^{l+1} + FFN(x_i'^{l+1})) \quad (10)$$

where H is the number of attention heads, \parallel denotes concatenation, d is the hidden dimension, d_i are node degrees, $W_{h,\mathcal{V}}^l \in \mathbb{R}^{\frac{d}{H} \times d_{\mathcal{V}}}$, $W_{h,\mathcal{E}}^l \in \mathbb{R}^{\frac{d}{H} \times d_{\mathcal{E}}}$, $\theta_1 \in \mathbb{R}^d$ and $\theta_2 \in \mathbb{R}^d$ are learnable weights (biases omitted for clarity), BN denotes Batch Normalization while FFN denotes a feed-forward network. We set ϕ_1^l and ϕ_2^l to be two-layer MLPs in all our experiments.

As in Kreuzer et al. [2021], we do not propagate edge features due to the added complexity and marginal benefits in performance. Further, we found degree scaling followed by batch normalization to be highly effective in incorporating node-degree information, as reported in Ma et al. [2023]. The final architecture of a layer of our proposed graph transformer, dubbed Eigenformer is illustrated in Figure 2b along with the attention mechanism in Figure 2a.

4 Experimental Results

We evaluate our proposed architecture on four benchmarks from the widely used Benchmarking GNNs work in Dwivedi et al. [2020], viz. ZINC, MNIST, PATTERN and CLUSTER. These four datasets include different graph learning objectives like node classification, graph classification and graph regression. They also cover widely different domains ranging from chemistry and computer vision to synthetically generated graphs. Further, we report numbers on two benchmarks from the Long-Range Graph Benchmark (LRGB) [Dwivedi et al., 2022b] to gauge how well our approach does in capturing long-range dependencies. We believe there is room for improvement in the reported results through a more extensive hyperparameter search when more training resources are available. Further details about the experimental setup can be found in appendix B.

Table 2: Test performance on two benchmarks from long-range graph benchmarks (LRGB) [Dwivedi et al., 2022b]. Due to limited training budget, we only show our results for a single training run while other baselines report mean \pm standard deviation numbers of 4 runs with different random seeds. Color codes denote top **first**, **second**, **third** results.

| Model | Peptides-func | Peptides-struct |
|--------------------|-------------------------------------|-------------------------------------|
| | AP \uparrow | MAE \downarrow |
| GCN | 0.5930 \pm 0.0023 | 0.3496 \pm 0.0013 |
| GINE | 0.5498 \pm 0.0079 | 0.3547 \pm 0.0045 |
| GatedGCN | 0.5864 \pm 0.0035 | 0.3420 \pm 0.0013 |
| GatedGCN+RWSE | 0.6069 \pm 0.0035 | 0.3357 \pm 0.0006 |
| Transformer+LapPE | 0.6326 \pm 0.0126 | 0.2529\pm0.0016 |
| SAN+LapPE | 0.6384 \pm 0.0121 | 0.2683 \pm 0.0043 |
| SAN+RWSE | 0.6439 \pm 0.0075 | 0.2545 \pm 0.0012 |
| GPS | 0.6535\pm0.0041 | 0.2500 \pm 0.0012 |
| GRIT | 0.6988\pm0.0082 | 0.2460\pm0.0012 |
| EXPHORMER | 0.6527 \pm 0.0043 | 0.2481\pm0.0007 |
| Eigenformer (ours) | 0.6234 | 0.2749 |

Baselines: We compare our method to different SOTA GNN methods including (hybrid) Graph Transformers: GraphGPS Rampásek et al. [2022], GRIT Ma et al. [2023], EGT Hussain et al. [2022], SAN Kreuzer et al. [2021], Graphormer Ying et al. [2021], K-Subgraph SAT Chen et al. [2022b] and EXPHORMER Shirzad et al. [2023], MP-GNNs: GCN Kipf and Welling [2017], GAT Veličković et al. [2018], GIN Xu et al. [2019], PNA Corso et al. [2020], GatedGCN Bresson and Laurent [2018], DGN Beaini et al. [2021], GSN Bouritsas et al. [2023] and other performant models like CIN Bodnar et al. [2021], CRaW1 Tönshoff et al. [2021] and GIN-AK+ Zhao et al. [2021].

Benchmarking GNNs [Dwivedi et al., 2020]: Table 1 compares our results to the baseline methods under the parameter budget used in Rampásek et al. [2022] (\sim 500K parameters for ZINC, PATTERN and CLUSTER, \sim 100K parameters for MNIST). Eigenformer routinely beats SOTA MP-GNNs and

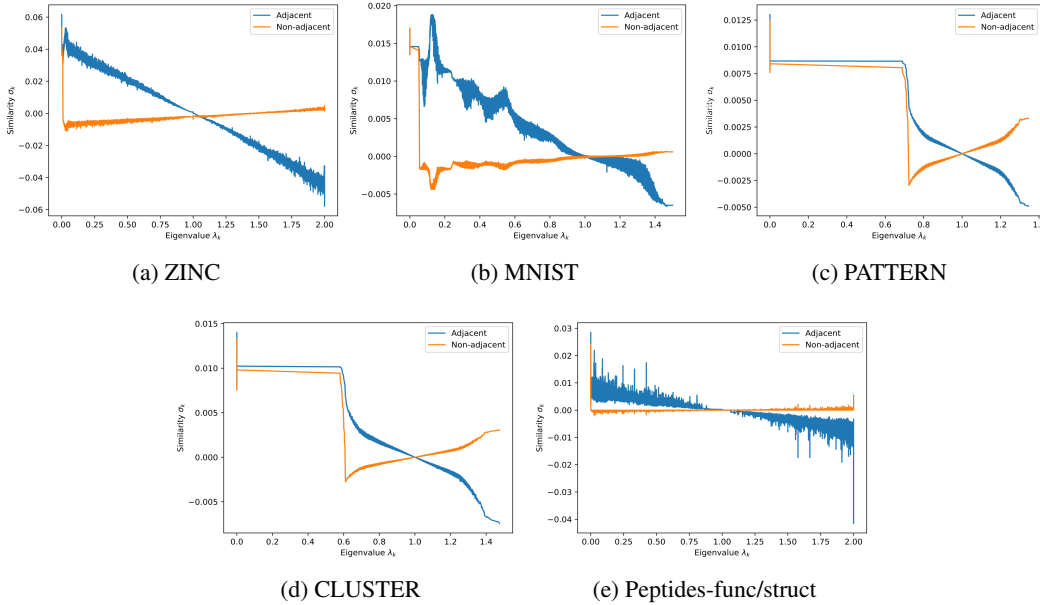


Figure 3: (Smoothed) similarity σ_k vs eigenvalue λ_k for adjacent and non-adjacent nodes

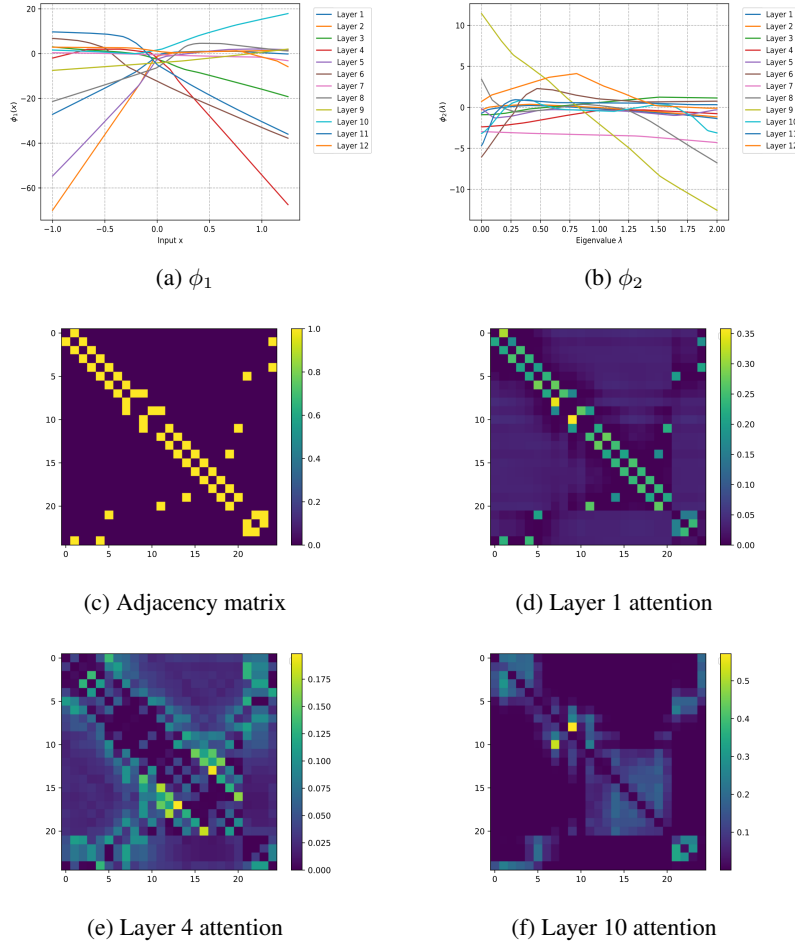


Figure 4: ϕ_1 , ϕ_2 and attention matrices for an example graph from ZINC dataset

approaches the performance of popular Graph Transformers that use different PEs like SAN [Kreuzer et al., 2021], Subgraph-SAT [G et al., 2023], Graphormer [Ying et al., 2021] etc. On the PATTERN dataset, we set a new benchmark with the best accuracy among all compared models.

Long-range graph benchmark [Dwivedi et al., 2022b]: To evaluate the ability to learn long-range dependencies, we report numbers on two benchmarks from the LRGB work [Dwivedi et al., 2022b] viz. Peptides-func (10-label graph classification) and Peptides-struct (11-task graph regression) in Table 2. Again, Eigenformer beats all the MP-GNN models easily and is competitive with the SOTA Transformers demonstrating its ability to capture long-range interactions in graph data.

Visualization of node similarities: It is instructive to visualize the difference in the distribution of similarities (defined in 4) between adjacent and non-adjacent nodes. Figure 3 shows the (smoothed) average similarity distribution w.r.t frequency for all datasets used in our work. On average, adjacent nodes have higher similarities at the lower end of the spectrum which change inversely with frequency. Non-adjacent nodes on the other hand have smaller similarities at smaller frequencies which rise towards the higher end of the spectrum. We posit that these distributional differences allow the attention mechanism to learn to discern local connections from long-range connections.

Visualization of ϕ_1 , ϕ_2 and attention matrices: Figures 4a and 4b show the learned functions ϕ_1^l and ϕ_2^l for $l = 1, \dots, 12$ for the ZINC dataset. The non-linear functions learnt by the model are most likely to ensure that the attention matrix focuses on the required connections/neighborhood as explained in the proof of Proposition 1. For example, Figure 4d shows the learned Layer 1 attention matrix for an example graph, which apparently tries to focus more on the 1-hop neighborhood interactions similar to the adjacency matrix shown in Figure 4c. Figure 4f showing Layer 10 attention on the other hand,

seems to focus on a larger (~ 5 -hop) neighborhood. Finally, as the complex interaction attention matrix in Figure 4e shows, k -hop neighbor interactions are not the only ones representable by our proposed attention mechanism.

5 Conclusion

Observing the wide variety of positional encoding schemes for Graph Transformers in the literature, we asked the question whether such encodings are essential to achieve graph representational learning objectives. We introduced a novel spectrum-aware attention (SAA) mechanism that incorporates structural graph inductive biases while remaining flexible enough to learn from features in the data. We proposed Eigenformer, a Graph Transformer with SAA at its core, that can be used for a variety of graph learning objectives with different task-specific heads. We empirically test the feasibility of our method through experiments on a number of common GNN benchmarks and find that it performs comparably to many popular GNN techniques using different schemes for PE generation, even beating the state-of-the-art on the PATTERN node-classification benchmark.

Several open challenges remain however, including computational complexity of the SAA mechanism with its $O(N^3)$ space and compute requirements. Recent work on sparse Graph Transformers using expander graphs and sparse attention with virtual/global nodes [Shirzad et al., 2023] along with the use of a subset of frequencies rather than the whole spectrum, may alleviate these issues. We hope this work provides the impetus to the broader graph-representational learning research community to pursue the development of other GNN architectures without the use of PEs.

References

- Petar Veličković. Everything is connected: Graph neural networks. *Current Opinion in Structural Biology*, 79:102538, 2023. ISSN 0959-440X. doi: <https://doi.org/10.1016/j.sbi.2023.102538>. URL <https://www.sciencedirect.com/science/article/pii/S0959440X2300012X>.
- Joan Bruna, Wojciech Zaremba, Arthur Szlam, and Yann LeCun. Spectral networks and locally connected networks on graphs. In Yoshua Bengio and Yann LeCun, editors, *2nd International Conference on Learning Representations, ICLR 2014, Banff, AB, Canada, April 14-16, 2014, Conference Track Proceedings*, 2014. URL <http://arxiv.org/abs/1312.6203>.
- Justin Gilmer, Samuel S. Schoenholz, Patrick F. Riley, Oriol Vinyals, and George E. Dahl. Neural message passing for quantum chemistry. In *Proceedings of the 34th International Conference on Machine Learning - Volume 70, ICML’17*, page 1263–1272. JMLR.org, 2017.
- Ashish Vaswani, Noam Shazeer, Niki Parmar, Jakob Uszkoreit, Llion Jones, Aidan N. Gomez, Lukasz Kaiser, and Illia Polosukhin. Attention is all you need. *CoRR*, abs/1706.03762, 2017. URL <http://arxiv.org/abs/1706.03762>.
- Vijay Prakash Dwivedi and Xavier Bresson. A generalization of transformer networks to graphs. *CoRR*, abs/2012.09699, 2020. URL <https://arxiv.org/abs/2012.09699>.
- Devin Kreuzer, Dominique Beaini, William L. Hamilton, Vincent Létourneau, and Prudencio Tossou. Rethinking graph transformers with spectral attention. *CoRR*, abs/2106.03893, 2021. URL <https://arxiv.org/abs/2106.03893>.
- Dexiong Chen, Leslie O’Bray, and Karsten M. Borgwardt. Structure-aware transformer for graph representation learning. In *International Conference on Machine Learning*, 2022a. URL <https://api.semanticscholar.org/CorpusID:246634635>.
- Chengxuan Ying, Tianle Cai, Shengjie Luo, Shuxin Zheng, Guolin Ke, Di He, Yanming Shen, and Tie-Yan Liu. Do transformers really perform badly for graph representation? In A. Beygelzimer, Y. Dauphin, P. Liang, and J. Wortman Vaughan, editors, *Advances in Neural Information Processing Systems*, 2021. URL <https://openreview.net/forum?id=OeWooOxFwDa>.
- Ladislav Rampášek, Michael Galkin, Vijay Prakash Dwivedi, Anh Tuan Luu, Guy Wolf, and Dominique Beaini. Recipe for a general, powerful, scalable graph transformer. In S. Koyejo, S. Mohamed, A. Agarwal, D. Belgrave, K. Cho, and A. Oh, editors, *Advances in Neural Information Processing Systems*, volume 35, pages 14501–14515. Curran Associates, Inc., 2022. URL https://proceedings.neurips.cc/paper_files/paper/2022/file/5d4834a159f1547b267a05a4e2b7cf5e-Paper-Conference.pdf.

- Md Shamim Hussain, Mohammed J. Zaki, and Dharmashankar Subramanian. Global self-attention as a replacement for graph convolution. In *Proceedings of the 28th ACM SIGKDD Conference on Knowledge Discovery and Data Mining*, KDD '22, page 655–665, New York, NY, USA, 2022. Association for Computing Machinery. ISBN 9781450393850. doi: 10.1145/3534678.3539296. URL <https://doi.org/10.1145/3534678.3539296>.
- Bohang Zhang, Shengjie Luo, Liwei Wang, and Di He. Rethinking the expressive power of GNNs via graph biconnectivity. In *The Eleventh International Conference on Learning Representations*, 2023. URL <https://openreview.net/forum?id=r9hNv76KoT3>.
- Uri Alon and Eran Yahav. On the bottleneck of graph neural networks and its practical implications. In *International Conference on Learning Representations*, 2021. URL <https://openreview.net/forum?id=i800Ph0CVH2>.
- Jake Topping, Francesco Di Giovanni, Benjamin Paul Chamberlain, Xiaowen Dong, and Michael M. Bronstein. Understanding over-squashing and bottlenecks on graphs via curvature. In *International Conference on Learning Representations*, 2022. URL <https://openreview.net/forum?id=7UmjRGzp-A>.
- Qimai Li, Zhichao Han, and Xiao-Ming Wu. Deeper insights into graph convolutional networks for semi-supervised learning. In *Proceedings of the Thirty-Second AAAI Conference on Artificial Intelligence and Thirtieth Innovative Applications of Artificial Intelligence Conference and Eighth AAAI Symposium on Educational Advances in Artificial Intelligence*, AAAI'18/AAAI'18/EAAI'18. AAAI Press, 2018. ISBN 978-1-57735-800-8.
- Kenta Oono and Taiji Suzuki. Graph neural networks exponentially lose expressive power for node classification. In *International Conference on Learning Representations*, 2020. URL <https://openreview.net/forum?id=S11d02EFPr>.
- Keyulu Xu, Weihua Hu, Jure Leskovec, and Stefanie Jegelka. How powerful are graph neural networks? In *International Conference on Learning Representations*, 2019. URL <https://openreview.net/forum?id=ryGs6iA5Km>.
- Andreas Loukas. What graph neural networks cannot learn: depth vs width. In *International Conference on Learning Representations*, 2020. URL <https://openreview.net/forum?id=B112bp4YwS>.
- Christopher Morris, Martin Ritzert, Matthias Fey, William L. Hamilton, Jan Eric Lenssen, Gaurav Rattan, and Martin Grohe. Weisfeiler and leman go neural: higher-order graph neural networks. In *Proceedings of the Thirty-Third AAAI Conference on Artificial Intelligence and Thirty-First Innovative Applications of Artificial Intelligence Conference and Ninth AAAI Symposium on Educational Advances in Artificial Intelligence*, AAAI'19/AAAI'19/EAAI'19. AAAI Press, 2019. ISBN 978-1-57735-809-1. doi: 10.1609/aaai.v33i01.33014602. URL <https://doi.org/10.1609/aaai.v33i01.33014602>.
- Derek Lim, Joshua David Robinson, Lingxiao Zhao, Tess Smidt, Suvrit Sra, Haggai Maron, and Stefanie Jegelka. Sign and basis invariant networks for spectral graph representation learning. In *The Eleventh International Conference on Learning Representations*, 2023. URL <https://openreview.net/forum?id=Q-UHqMorzil>.
- Vijay Prakash Dwivedi, Anh Tuan Luu, Thomas Laurent, Yoshua Bengio, and Xavier Bresson. Graph neural networks with learnable structural and positional representations. In *International Conference on Learning Representations*, 2022a. URL <https://openreview.net/forum?id=wTTjnvGphYj>.
- Liheng Ma, Chen Lin, Derek Lim, Adriana Romero-Soriano, Puneet K. Dokania, Mark Coates, Philip H.S. Torr, and Ser-Nam Lim. Graph inductive biases in transformers without message passing. In *Proceedings of the 40th International Conference on Machine Learning*, ICML'23. JMLR.org, 2023.
- Yuan Li, Xiaodan Liang, Zhiting Hu, Yinbo Chen, and Eric P. Xing. Graph transformer, 2019. URL <https://openreview.net/forum?id=HJei-2RcK7>.
- Jiawei Zhang, Haopeng Zhang, Li Sun, and Congying Xia. Graph-bert: Only attention is needed for learning graph representations. *ArXiv*, abs/2001.05140, 2020. URL <https://api.semanticscholar.org/CorpusID:210698881>.
- Grégoire Mialon, Dexiong Chen, Margot Selosse, and Julien Mairal. Graphit: Encoding graph structure in transformers. *ArXiv*, abs/2106.05667, 2021. URL <https://api.semanticscholar.org/CorpusID:235390675>.
- Dexiong Chen, Laurent Jacob, and Julien Mairal. Convolutional kernel networks for graph-structured data. In *Proceedings of the 37th International Conference on Machine Learning*, ICML'20. JMLR.org, 2020.

- Gabriele Corso, Luca Cavalleri, Dominique Beaini, Pietro Liò, and Petar Velickovic. Principal neighbourhood aggregation for graph nets. In *Proceedings of the 34th International Conference on Neural Information Processing Systems, NIPS'20*, Red Hook, NY, USA, 2020. Curran Associates Inc. ISBN 9781713829546.
- Dexiong Chen, Leslie O’Bray, and Karsten M. Borgwardt. Structure-aware transformer for graph representation learning. In *International Conference on Machine Learning*, 2022b. URL <https://api.semanticscholar.org/CorpusID:246634635>.
- Sumedh B G, Sanjay Patnala, Himil Vasava, Akshay Sethi, and Sonia Gupta. SATG : Structure aware transformers on graphs for node classification. In *NeurIPS 2023 Workshop: New Frontiers in Graph Learning*, 2023. URL <https://openreview.net/forum?id=EVp40Cz0PR>.
- Romain Menegaux, Emmanuel Jehanno, Margot Selosse, and Julien Mairal. Self-attention in colors: Another take on encoding graph structure in transformers. *Transactions on Machine Learning Research*, 2023. ISSN 2835-8856. URL <https://openreview.net/forum?id=3dQCNqqv2d>.
- Yaron Lipman, Raif M. Rustamov, and Thomas A. Funkhouser. Biharmonic distance. *ACM Trans. Graph.*, 29(3), jul 2010. ISSN 0730-0301. doi: 10.1145/1805964.1805971. URL <https://doi.org/10.1145/1805964.1805971>.
- Ronald R. Coifman and Stéphane Lafon. Diffusion maps. *Applied and Computational Harmonic Analysis*, 21(1):5–30, 2006. ISSN 1063-5203. doi: <https://doi.org/10.1016/j.acha.2006.04.006>. URL <https://www.sciencedirect.com/science/article/pii/S1063520306000546>. Special Issue: Diffusion Maps and Wavelets.
- Michael M. Bronstein, Joan Bruna, Yann LeCun, Arthur Szlam, and Pierre Vandergheynst. Geometric deep learning: Going beyond euclidean data. *IEEE Signal Processing Magazine*, 34(4):18–42, 2017. doi: 10.1109/MSP.2017.2693418.
- Vijay Prakash Dwivedi, Chaitanya K. Joshi, Thomas Laurent, Yoshua Bengio, and Xavier Bresson. Benchmarking graph neural networks. *CoRR*, abs/2003.00982, 2020. URL <https://arxiv.org/abs/2003.00982>.
- Vijay Prakash Dwivedi, Ladislav Rampásek, Michael Galkin, Ali Parviz, Guy Wolf, Anh Tuan Luu, and Dominique Beaini. Long range graph benchmark. In S. Koyejo, S. Mohamed, A. Agarwal, D. Belgrave, K. Cho, and A. Oh, editors, *Advances in Neural Information Processing Systems*, volume 35, pages 22326–22340. Curran Associates, Inc., 2022b. URL https://proceedings.neurips.cc/paper_files/paper/2022/file/8c3c666820ea055a77726d66fc7d447f-Paper-Datasets_and_Benchmarks.pdf.
- Hamed Shirzad, Ameya Velingker, Balaji Venkatachalam, Danica J. Sutherland, and Ali Kemal Sinop. Exphormer: sparse transformers for graphs. In *Proceedings of the 40th International Conference on Machine Learning, ICML’23*. JMLR.org, 2023.
- Thomas N. Kipf and Max Welling. Semi-supervised classification with graph convolutional networks. In *International Conference on Learning Representations*, 2017. URL <https://openreview.net/forum?id=SJU4ayYgl>.
- Petar Veličković, Guillem Cucurull, Arantxa Casanova, Adriana Romero, Pietro Liò, and Yoshua Bengio. Graph attention networks. In *International Conference on Learning Representations*, 2018. URL <https://openreview.net/forum?id=rJXMpikCZ>.
- Xavier Bresson and Thomas Laurent. Residual gated graph convnets, 2018. URL <https://openreview.net/forum?id=HyXBcYg0b>.
- Dominique Beaini, Saro Passaro, Vincent Letourneau, William L. Hamilton, Gabriele Corso, and Pietro Liò. Directional graph networks, 2021. URL <https://openreview.net/forum?id=FUdBF49WRV1>.
- Giorgos Bouritsas, Fabrizio Frasca, Stefanos Zafeiriou, and Michael M. Bronstein. Improving graph neural network expressivity via subgraph isomorphism counting. *IEEE Transactions on Pattern Analysis and Machine Intelligence*, 45(1):657–668, 2023. doi: 10.1109/TPAMI.2022.3154319.
- Cristian Bodnar, Fabrizio Frasca, Yu Guang Wang, Nina Otter, Guido Montúfar, Pietro Lio’, and Michael M. Bronstein. Weisfeiler and lehman go topological: Message passing simplicial networks. *ArXiv*, abs/2103.03212, 2021. URL <https://api.semanticscholar.org/CorpusID:232110693>.
- Jan Tönshoff, Martin Ritzert, Hinrikus Wolf, and Martin Grohe. Graph learning with 1d convolutions on random walks. *ArXiv*, abs/2102.08786, 2021. URL <https://api.semanticscholar.org/CorpusID:263883878>.

Lingxiao Zhao, Wei Jin, Leman Akoglu, and Neil Shah. From stars to subgraphs: Uplifting any gnn with local structure awareness. *ArXiv*, abs/2110.03753, 2021. URL <https://api.semanticscholar.org/CorpusID:238531375>.

Kurt Hornik, Maxwell Stinchcombe, and Halbert White. Multilayer feedforward networks are universal approximators. *Neural Networks*, 2(5):359–366, 1989. ISSN 0893-6080. doi: [https://doi.org/10.1016/0893-6080\(89\)90020-8](https://doi.org/10.1016/0893-6080(89)90020-8). URL <https://www.sciencedirect.com/science/article/pii/0893608089900208>.

A Proof of Proposition 1

(1) For an undirected graph $\mathcal{G} = (\mathcal{V}, \mathcal{E})$ with adjacency matrix A and degree matrix D , we have:

$$L_{sym} = I - D^{-\frac{1}{2}} A D^{-\frac{1}{2}} = I - A_{sym}$$

Since L_{sym} is real and symmetric, it admits an eigendecomposition as follows:

$$L_{sym} = U \Lambda U^{-1}$$

where the columns of $U = [u_1, u_2, \dots, u_{|\mathcal{V}|}]$ are the right eigenvectors of L_{sym} . It follows that,

$$A_{sym} = I - U \Lambda U^{-1} = U(I - \Lambda)U^{-1} = \sum_{i=1}^{|\mathcal{V}|} u_i u_i^T (1 - \lambda_i) \quad (11)$$

Thus, in general we have:

$$\sum_{k=0}^m \theta_k A_{sym}^k = \sum_{i=1}^{|\mathcal{V}|} u_i u_i^T \sum_{k=0}^m \theta_k (1 - \lambda_i)^k \quad (12)$$

The continuous functions $\phi_1(x) = x$ and $\phi_2(\lambda) = \sum_{k=0}^m \theta_k (1 - \lambda)^k$ in 5 can hence be approximated to an arbitrary accuracy by sufficiently wide MLPs by virtue of standard universal approximation results [Hornik et al., 1989].

(2) We need to prove that there exist functions ϕ_1 and ϕ_2 such that $\phi_1(\sum_{k=1}^n \sigma_k^g[i, j] \cdot \phi_2(\lambda_k^g)) \approx SPD^g[i, j]$ for every graph g with adjacency matrix $A \in \mathbb{G}_n$ and every node-pair (i, j) in g .

If we can ensure that we can choose ϕ_2 such that it is possible to map every value $\sum_{k=1}^n \sigma_k^g[i, j] \cdot \phi_2(\lambda_k^g)$ to the unique value $SPD^g[i, j]$, then we can simply define $\phi_1 : \mathbb{R} \rightarrow \mathbb{R}$ as the piecewise-linear continuous function:

$$\phi_1\left(\sum_{k=1}^n \sigma_k^g[i, j] \cdot \phi_2(\lambda_k^g)\right) = \phi_1\left(\sum_{k=1}^n u_k^g[i] u_k^g[j] \cdot \phi_2(\lambda_k^g)\right) = SPD^g[i, j] \quad (13)$$

which can be approximated by a sufficiently wide MLP. The proof then amounts to showing the existence of such a ϕ_2 .

Notation: With a slight abuse of notation, let $v_{ij}^g = [u_1^g[i] u_1^g[j], u_2^g[i] u_2^g[j], \dots, u_n^g[i] u_n^g[j]]^T$. Further denote by ϕ_2^g the vector $[\phi_2(\lambda_1^g), \dots, \phi_2(\lambda_n^g)]^T$, so that $\sum_{k=1}^n u_k^g[i] u_k^g[j] \cdot \phi_2(\lambda_k^g) = v_{ij}^{gT} \phi_2^g$.

Now, let $\phi_2(\lambda) = \sum_{k=0}^m \theta_k (1 - \lambda)^k$ for some $m \in \mathbb{Z}$.

Case 1: $v_{ij}^g = v_{pq}^g$ for some graph g and node-pairs (i, j) and (p, q) in g .

In this case, by virtue of 12, $SPD^g[i, j] = SPD^g[p, q]$ since $A_{sym}^k[i, j] = A_{sym}^k[p, q]$, which implies that there is a k -hop path from i to j iff there is a k -hop path from p to q . Moreover, in this case $v_{ij}^{gT} \phi_2^g = v_{pq}^{gT} \phi_2^g$.

Case 2: $v_{ij}^g \neq v_{pq}^g$ for some graph g and node-pairs (i, j) and (p, q) in g .

If $SPD^g[i, j] = SPD^g[p, q]$, we simply set $\phi_1(v_{ij}^{gT} \phi_2^g) = SPD^g[i, j]$ and $\phi_1(v_{pq}^{gT} \phi_2^g) = SPD^g[p, q]$.

If $SPD^g[i, j] \neq SPD^g[p, q]$ and $v_{ij}^{gT} \phi_2^g \neq v_{pq}^{gT} \phi_2^g$, we are done. If however, $v_{ij}^{gT} \phi_2^g = v_{pq}^{gT} \phi_2^g$, choose an index r such that $v_{ij}^g[r] \neq v_{pq}^g[r]$. We can then perturb θ_r such that $v_{ij}^{gT} \phi_2^g$ becomes unequal to $v_{pq}^{gT} \phi_2^g$, in which case we again can set $\phi_1(v_{ij}^{gT} \phi_2^g) = SPD^g[i, j]$ and $\phi_1(v_{pq}^{gT} \phi_2^g) = SPD^g[p, q]$. We are assured that such a perturbation exists without violating the continuity constraints of ϕ_1 in 13 for other graphs and node-pairs in \mathbb{G}_n .

Case 3: $v_{ij}^{g_1} = v_{pq}^{g_2}$ for some graphs g_1, g_2 and node-pairs (i, j) in g_1 and (p, q) in g_2 .

If $SPD^{g_1}[i, j] = SPD^{g_2}[p, q]$, we simply set $\phi_1(v_{ij}^{g_1 T} \phi_2^{g_1}) = SPD^{g_1}[i, j]$ and $\phi_1(v_{pq}^{g_2 T} \phi_2^{g_2}) = SPD^{g_2}[p, q]$.

If $SPD^g[i, j] \neq SPD^g[p, q]$ and $v_{ij}^{g_1 T} \phi_2^{g_1} \neq v_{pq}^{g_2 T} \phi_2^{g_2}$, we are done. If however, $v_{ij}^{g_1 T} \phi_2^{g_1} = v_{pq}^{g_2 T} \phi_2^{g_2}$, choose an index r such that $\lambda_r^{g_1} \neq \lambda_r^{g_2}$ (which exists necessarily since otherwise $SPD^{g_1}[i, j] = SPD^{g_2}[p, q]$ due to 12). We can then perturb θ_r such that $v_{ij}^{g_1 T} \phi_2^{g_1}$ becomes unequal to $v_{pq}^{g_2 T} \phi_2^{g_2}$, in which case we again can set $\phi_1(v_{ij}^{g_1 T} \phi_2^{g_1}) = SPD^{g_1}[i, j]$ and $\phi_1(v_{pq}^{g_2 T} \phi_2^{g_2}) = SPD^{g_2}[p, q]$. Similarly to Case 2 above, we are assured that such a perturbation exists without violating the continuity constraints of ϕ_1 in 13 for other graphs and node-pairs in \mathbb{G}_n .

Case 4: $v_{ij}^{g_1} \neq v_{pq}^{g_2}$ for some graphs g_1, g_2 and node-pairs (i, j) in g_1 and (p, q) in g_2 .

If $SPD^{g_1}[i, j] = SPD^{g_2}[p, q]$, we simply set $\phi_1(v_{ij}^{g_1 T} \phi_2^{g_1}) = SPD^{g_1}[i, j]$ and $\phi_1(v_{pq}^{g_2 T} \phi_2^{g_2}) = SPD^{g_2}[p, q]$.

If $SPD^g[i, j] \neq SPD^g[p, q]$ and $v_{ij}^{g_1 T} \phi_2^{g_1} \neq v_{pq}^{g_2 T} \phi_2^{g_2}$, we are done. If however, $v_{ij}^{g_1 T} \phi_2^{g_1} = v_{pq}^{g_2 T} \phi_2^{g_2}$, choose an index r such that $v_{ij}^{g_1}[r] \neq v_{pq}^{g_2}[r]$. We can then perturb θ_r such that $v_{ij}^{g_1 T} \phi_2^{g_1}$ becomes unequal to $v_{pq}^{g_2 T} \phi_2^{g_2}$, in which case we again can set $\phi_1(v_{ij}^{g_1 T} \phi_2^{g_1}) = SPD^{g_1}[i, j]$ and $\phi_1(v_{pq}^{g_2 T} \phi_2^{g_2}) = SPD^{g_2}[p, q]$. Similarly to Case 2 and 3 above, we are assured that such a perturbation exists without violating the continuity constraints of ϕ_1 in 13 for other graphs and node-pairs in \mathbb{G}_n since the set of such constraints is finite and bounded.

Thus, we have proven that the continuous function $\phi_2(\lambda) = \sum_{k=0}^m \theta_k (1 - \lambda)^k$ for some $m \in \mathbb{Z}$ can be chosen to ensure the continuity of ϕ_1 defined in 13. Both functions can hence be approximated by MLPs to an arbitrary accuracy due to Hornik et al. [1989].

B Experiment Details

B.1 Description of Datasets

Details specific to each dataset used in our results are presented in Table 3.

Table 3: Overview of datasets used in our work

| Dataset | #graphs | #nodes | #edges | Directed | Prediction Task |
|-----------------|---------|--------------|---------------|----------|-------------------------------|
| ZINC | 12,000 | ~ 23.2 | ~ 24.9 | No | Graph regression |
| MNIST | 70,000 | ~ 70.6 | ~ 564.5 | No | 10-class Graph classification |
| PATTERN | 14,000 | ~ 118.9 | ~ 3039.3 | No | Binary node classification |
| CLUSTER | 12,000 | ~ 117.2 | ~ 2150.9 | No | 6-class Node classification |
| Peptides-func | 15,535 | ~ 150.9 | ~ 307.3 | No | 10-label Graph classification |
| Peptides-struct | 15,535 | ~ 150.9 | ~ 307.3 | No | 11-task Graph regression |

B.2 Hyperparameters

Due to a limited training budget we could not perform a large scale hyperparameter search and mostly borrowed configurations from Ma et al. [2023] and Rampásek et al. [2022], keeping in line with the parameter budgets, optimizer (AdamW with $\text{betas} = (0.9, 0.99)$ and $\text{eps} = 1e - 8$) and learning rate schedule (warmup+cosine annealing) used therein. However, our experiments show that due to a very different attention mechanism, our method benefits from deeper and wider models, and lower dropout rates. More details are included in Table 4 and 5.

B.3 Hardware resources

All experiments were carried out on an AWS ml.g5.2xlarge Sagemaker training instance with 32 GB of system RAM and a single NVIDIA A10G GPU with 24GB of VRAM.

Table 4: Best hyperparameter configurations for the benchmarks from Dwivedi et al. [2020]

| Hyperparameter | ZINC | MNIST | PATTERN | CLUSTER |
|------------------------|--------|-------|---------|---------|
| # Transformer Layers | 12 | 3 | 10 | 16 |
| # Heads | 8 | 8 | 8 | 8 |
| Node feature embedding | 128 | - | - | - |
| Edge feature embedding | 128 | - | - | - |
| Hidden dim | 80 | 72 | 96 | 80 |
| ϕ_1 Hidden dim | 80 | 72 | 104 | 80 |
| ϕ_2 Hidden dim | 80 | 72 | 104 | 72 |
| Dropout | 0 | 0 | 0 | 0 |
| Attention dropout | 0.2 | 0.1 | 0.1 | 0.1 |
| Graph pooling | sum | mean | - | - |
| Batch size | 128 | 512 | 32 | 32 |
| Learning rate | 0.001 | 0.001 | 0.0005 | 0.0005 |
| # Epochs | 2000 | 200 | 100 | 100 |
| # Warmup epochs | 50 | 5 | 5 | 5 |
| Weight decay | 1e-5 | 1e-5 | 1e-5 | 1e-5 |
| # Parameters | 496713 | 97360 | 504885 | 507590 |

Table 5: Best hyperparameter configurations for the benchmarks from Dwivedi et al. [2022b]

| Hyperparameter | Peptides-func | Peptides-struct |
|----------------------|---------------|-----------------|
| # Transformer Layers | 10 | 10 |
| # Heads | 8 | 8 |
| Hidden dim | 96 | 96 |
| ϕ_1 Hidden dim | 80 | 80 |
| ϕ_2 Hidden dim | 80 | 80 |
| Dropout | 0 | 0 |
| Attention dropout | 0 | 0 |
| Graph pooling | mean | mean |
| Batch size | 8 | 8 |
| Learning rate | 0.0003 | 0.0003 |
| # Epochs | 200 | 200 |
| # Warmup epochs | 5 | 5 |
| Weight decay | 1e-5 | 1e-5 |
| # Parameters | 509406 | 509503 |